

$$\Delta E = \Delta E_{\text{ph.s.}} + \Delta E_{\text{bs}}, \quad (6.4)$$

where

$$\Delta E_{\text{ph.s.}} = -(2/\pi) \int_0^{E_m} \delta(E) dE \quad (6.5)$$

and

$$\Delta E_{\text{bs}} = N \sum_{i=1}^n \epsilon_i. \quad (6.6)$$

The contribution from the phase shift has an extra factor of 2, as compared to result (2.21), to allow for the two possible directions of electron spin. The factor  $N$  in bound-state contribution has a value of 1 or 2 depending upon whether it is occupied by one or two electrons. However, since this contribution is negligibly small, we can ignore this difference.

Studies were made for different potential strengths by just replacing  $V$  by  $\lambda V$ . Table III shows the results for four values of  $\lambda$ .

From the study of the single vacancy,<sup>3,4</sup> it was concluded that a value of  $\lambda = 1.04$  is required. The

change in the one-electron energy for this case is now found to be  $-0.67$  Ry. The corresponding value for the single vacancy<sup>4</sup> is  $1.67$  Ry. Thus we get a net change for a vacancy-interstitial formation of  $1.00$  Ry or  $13.6$  eV.

To evaluate the actual formation energy of the vacancy-interstitial pair, one has still to consider the change in the energy associated with the Coulomb interaction of electrons in the neighborhood of the vacancy and the interstitial and the lattice distortion in the two areas.

We searched for a possible bound state in the gap below the conduction bands. None was found. This can possibly explain the lack of direct evidence of the presence of an interstitial in silicon.

Further study on other possible interstitial locations is in progress.

#### ACKNOWLEDGMENT

The author would like to thank Professor J. Callaway for suggesting this problem and for many helpful discussions.

<sup>†</sup>Supported in part by the U.S. Air Force Office of Scientific Research under Grant No. AF 68-1565.

<sup>1</sup>J. Callaway, *J. Math. Phys.* **5**, 783 (1964).

<sup>2</sup>J. Callaway, *Phys. Rev.* **154**, 515 (1967).

<sup>3</sup>J. Callaway and A. J. Hughes, *Phys. Rev.* **156**, 860 (1967); **164**, 1043 (1967).

<sup>4</sup>J. Callaway, *Phys. Rev. B* **3**, 2556 (1971).

<sup>5</sup>D. Brust, *Phys. Rev.* **134**, A1337 (1964).

<sup>6</sup>W. A. Harrison, *Pseudopotentials in the Theory of*

*Metals* (Benjamin, New York, 1964).

<sup>7</sup>J. Callaway (private communication).

<sup>8</sup>S. P. Singhal, Louisiana State University Technical Report No. P-590/71, 1971 (unpublished).

<sup>9</sup>F. C. von der Lage and H. A. Bethe, *Phys. Rev.* **71**, 612 (1947).

<sup>10</sup>S. Ganesan and R. Srinivasan, *Can. J. Phys.* **40**, 1153 (1962); *Indian J. Pure Appl. Phys.* **1**, 282 (1963).

## Experimental Determination of the Electron Temperature from Burstein-Shift Experiments in Gallium Antimonide<sup>†</sup>

H. Heinrich\* and W. Jantsch

*Institut für Angewandte Physik der Universität Wien  
und Ludwig Boltzmann Institut für Festkörperphysik, Vienna, Austria*  
(Received 10 March 1971)

The shift of the Fermi energy because of an applied electric field is determined from Burstein-shift measurements in GaSb at 77 K up to field strengths of 150 V/cm. By comparison with results of the Burstein shift at lattice temperatures up to 105 K without an electric field, the electron temperature is obtained as a function of the electric field. Calculations of the electron temperature, based on a two-band model, are compared with the experimental results.

### I. INTRODUCTION

Hot-electron experiments in semiconductors with large electron concentrations are often interpreted by assuming a Maxwellian or a Fermi distribution function with an electron temperature  $T_e$ , which is

higher than the lattice temperature. Methods of an experimental determination of  $T_e$  from Shubnikov-de Haas measurements<sup>1</sup> and Raman scattering<sup>2</sup> due to hot electrons have been reported. However, Shubnikov-de Haas experiments are restricted to low temperatures and high magnetic fields, and

for the evaluation of the Raman effect an accurate knowledge of the band structure of the investigated material is necessary. In this paper we want to report a new method for the determination of  $T_e$  from Burstein-shift (BS) experiments.

In degenerate semiconductors the absorption edge is shifted to higher photon energies by an amount<sup>3</sup>

$$\epsilon_B = (1 + m_e/m_h) (\epsilon_F - 4kT_e), \quad (1)$$

where  $m_e$  and  $m_h$  are the effective masses of electrons and holes, respectively,  $\epsilon_F$  is the Fermi energy, and  $T_e$  the electron temperature.

Recently Shur<sup>4</sup> has pointed out that the BS may be influenced by an external electric field. For the fields considered here, the influence on the absorption edge may be expected to be several orders of magnitude greater than the Franz-Keldysh effect.<sup>5,6</sup> The electric field heats the electron gas and consequently reduces the Fermi energy and hence the BS. Transmitted light with a wavelength at the fundamental absorption edge therefore is modulated by an electric field. This light modulation is very fast; it occurs within the energy relaxation time which for GaSb at 77 K is approximately  $2 \times 10^{-11}$  sec.<sup>7</sup> As will be shown, the modulation is proportional to the field-induced decrease of  $\epsilon_B$  as long as  $\epsilon_F > 4kT_e$  [Eq. (1)]. For higher field strengths, when  $\epsilon_B$  in Eq. (1) becomes negative, the BS vanishes and the modulation saturates. Therefore the electron temperature may be determined for  $T_e < \epsilon_F/4k$  as a function of the applied electric field, if the dependence of the Fermi energy on the electron temperature,  $\epsilon_F(T_e)$ , is known. Since the shift in Fermi energy resulting from a variation of either the electron temperature or the lattice temperature is the same, the Fermi energy may be determined from measurements of the BS as a function of lattice

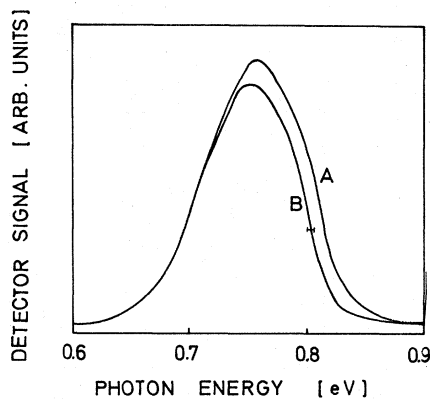


FIG. 1. Spectral dependence of the signal of a Ge detector obtained from transmission measurements on  $n$ -GaSb with an electron concentration of  $3.5 \times 10^{17}/\text{cm}^3$  (curve A), and  $6.8 \times 10^{16}/\text{cm}^3$  (curve B) at 77 K. The bar at 0.8 eV indicates the resolution of the monochromator.

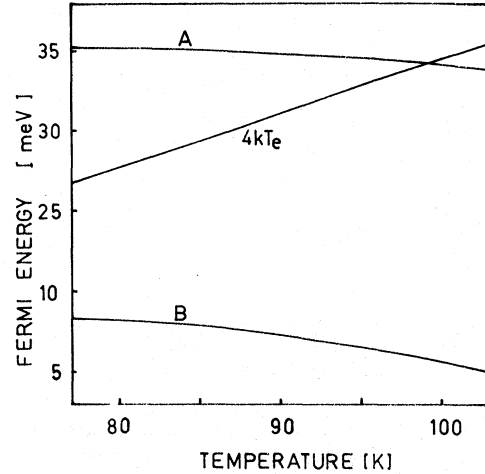


FIG. 2. Results for the Fermi energy calculated as a function of the temperature for GaSb with an electron concentration of  $3.5 \times 10^{17}/\text{cm}^3$  (curve A) and  $6.8 \times 10^{16}/\text{cm}^3$  (curve B). The straight line gives the energy  $4kT_e$ .

temperature.

## II. EXPERIMENTAL

Samples were prepared from Te-doped GaSb. Typical sample dimensions were  $2 \times 2 \times 0.08$  mm<sup>3</sup>. Carrier concentration and mobilities were determined from conductivity and Hall measurements at 77 K, where the population of the  $L_1$  minima, lying 0.09 eV above the  $\Gamma_1$  minimum, still is neg-

TABLE I. Constants used in the numerical calculation.

|  |  |
|--|--|
| $n = 3.5 \times 10^{17}/\text{cm}^3$                       | Carrier concentration of material of curve A <sup>a</sup>  |
| $\mu_0(77 \text{ K}) = 7000$<br>$\text{cm}^2/\text{V sec}$ | Mobility in $\Gamma_1$ of material of curve A <sup>a</sup> |
| $n = 6.8 \times 10^{16}/\text{cm}^3$                       | Carrier concentration of material of curve B <sup>a</sup>  |
| $\mu_0(77 \text{ K}) = 6900$<br>$\text{cm}^2/\text{V sec}$ | Mobility in $\Gamma_1$ of material of curve B <sup>a</sup> |
| $(\mu_0/\mu_1)_{77 \text{ K}} = 9.0$                       | Mobility ratio (Ref. 10)                                   |
| $m_0 = 0.05m_e$  | Effective mass in $\Gamma_1$ (Ref. 11)                     |
| $m_{1t} = 0.143m_e$  | Transverse effective mass in $L_1$ (Ref. 10)               |
| $K = 8.6$  | Anisotropy coefficient in $L_1$ (Ref. 11)                  |
| $\alpha = 56.5$  | Effective density of states ratio                          |
| $\Delta(77 \text{ K}) = 0.09 \text{ eV}$                   | Energy separation between $\Gamma_1$ and $L_1$ (Ref. 10)   |
| $\tau_e = 1.6 \times 10^{-11} \text{ sec}$                 | Energy relaxation time (Ref. 7)                            |

<sup>a</sup>Obtained from Hall and conductivity measurements.

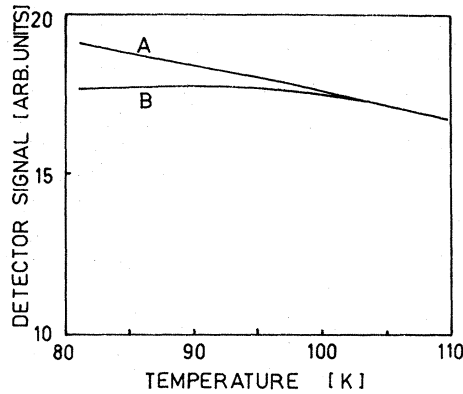


FIG. 3. Detector signals obtained from transmission measurements on degenerate (curve A) and nondegenerate (curve B) material as a function of the lattice temperature.

ligible. The results are given in Table I.

In Fig. 1 the detector signal obtained from transmission measurements is plotted as a function of the photon energy. The curves marked A and B were measured at 77 K with the help of a Ge-photovoltaic detector, curve A with *n*-type GaSb of an electron density of  $3.5 \times 10^{17}/\text{cm}^3$ , curve B with  $6.8 \times 10^{16}/\text{cm}^3$ . Because of the drop of the spectral sensitivity of the Ge detector below 0.75 eV, curves A and B show the same dispersion relation for the lower part of the spectrum.

A calculation of the Fermi energy, based on a two-band model as described in Ref. 8, exhibits that the material of curve B is not degenerate at 77 K. In this model carrier transfer from the lowest  $\Gamma_1$  conduction-band minimum to the  $L_1$  minima

is taken into account. Assuming a Fermi distribution function, the carrier concentrations  $n_0$  and  $n_1$  in the  $\Gamma_1$  and  $L_1$  valleys, respectively, are given by

$$n_0 = 4\pi \left( \frac{2m_0 k T_e}{h^2} \right)^{3/2} F_{1/2} \left( \frac{\epsilon_F}{k T_e} \right), \quad (2)$$

$$n_1 = 4\pi \left( \frac{2m_{1t} k T_e}{h^2} \right)^{3/2} 4K^{1/2} F_{1/2} \left( \frac{\epsilon_F - \Delta}{k T_e} \right), \quad (3)$$

where  $m_0$  is the effective mass in  $\Gamma_1$ ,  $K = m_{1t}/m_{1l}$  is the anisotropy coefficient for the  $L_1$  minima,  $\Delta$  is the energetic separation between these valleys, and  $F_{1/2}$  are Fermi integrals. Assuming the total carrier concentration  $n = n_0 + n_1$  to be constant, the Fermi energy is obtained by a numerical solution of Eqs. (2) and (3) as a function of the electron temperature. The constants used in the calculation are given in Table I and results for the total carrier concentrations of the investigated materials of curves A and B are shown in Fig. 2. According to Eq. (1) the difference of the Fermi energy and the energy  $4kT_e$  (straight line in Fig. 2) is proportional to the BS. For the material of curve A this difference, and hence the BS, vanishes at 99 K. At 77 K for  $\epsilon_F - 4kT_e$ , a value of 8.5 meV is obtained. The Fermi energy of the material of curve B is less than  $4kT$  even at 77 K and no BS occurs. Therefore the energetic separation of the curves A and B in Fig. 1, which is approximately 11 meV, corresponds to the BS of the higher-doped material.

For the investigation of the transmission depending on electric field and lattice temperature, polychromatic light has been used. When the band edge is shifted by an amount of  $\Delta\epsilon$  due to the change in

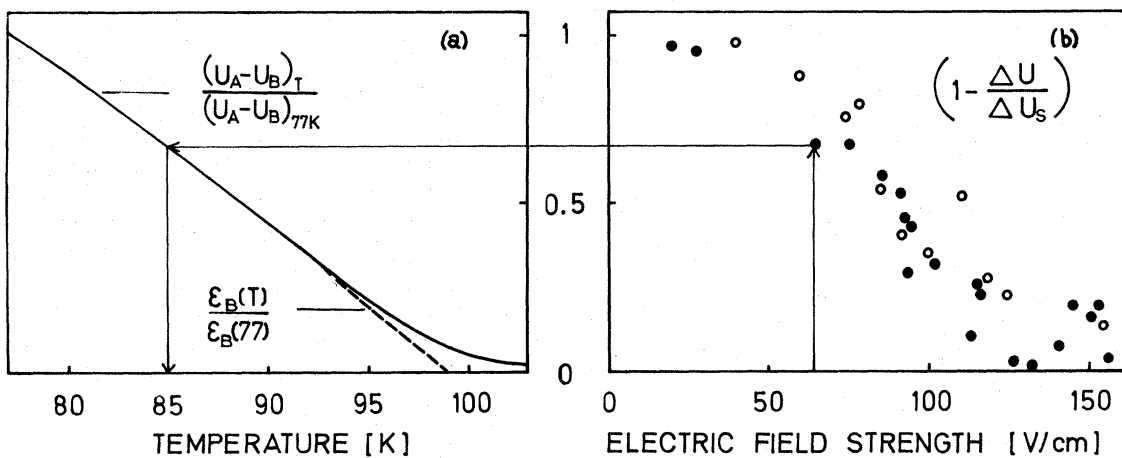


FIG. 4. (a) Temperature dependence of the difference in detector signal between sample of curves A and B normalized to 77 K (full line). Dashed line represents the calculated value of  $\epsilon_B(T)/\epsilon_B(77)$ . (b) Results for  $1 - \Delta U/\Delta U_s$  obtained from electric-field-dependent measurements (full and open circles were measured on 2 different samples).

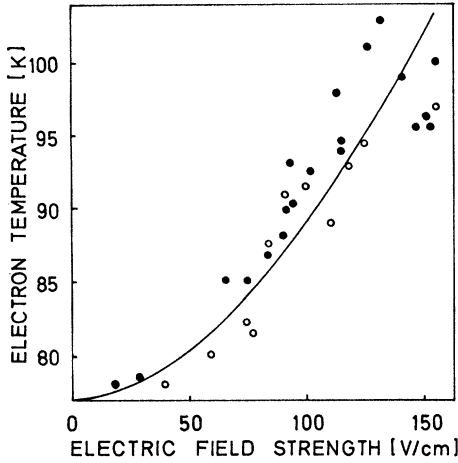


FIG. 5. Experimental (full and open circles) and calculated results (solid line) of the electron temperature as a function of the electric field strength.

BS, the transmittivity  $T_{\Delta\epsilon}(\epsilon)$  at a photon energy  $\epsilon$  equals  $T(\epsilon + \Delta\epsilon)$ ,  $T(\epsilon)$  being the transmittivity without shift. The corresponding change  $\Delta U$  in detector signal  $U$  may be described by

$$\Delta U = \int_0^{\infty} [T(\epsilon + \Delta\epsilon) - T(\epsilon)] S(\epsilon) d\epsilon, \quad (4)$$

where  $S(\epsilon)$  is the spectral sensitivity of the detector. The integrand in Eq. (4) can be expanded into a Taylor series, and terms of second and higher orders can be neglected, if

$$\left| \frac{1}{S} \frac{\partial S}{\partial \epsilon} \frac{\Delta\epsilon}{2} \right| \ll 1. \quad (5)$$

The value of Eq. (5) was determined to be less than 0.1 for the highest  $\Delta\epsilon$  under consideration. In this case the detector signal is proportional to  $\Delta\epsilon$ , from which the variation of  $\epsilon_F - 4kT$  is obtained.

In order to determine the BS as a function of the lattice temperature, the variation of the energy gap<sup>9</sup> with temperature had to be taken into account. In Fig. 3 the detector signals measured on the degenerate curve (A) and nondegenerate curve (B) samples are plotted as a function of the lattice temperature. Curve B represents the dependence of the energy gap on the lattice temperature. Above 100 K, when the BS of the material curve (A) vanishes, both curves depend in the same way on the temperature. The BS is obtained from the difference of the detector signals ( $U_A - U_B$ ). Normalized values of the BS as a function of the lattice temperature are given in Fig. 4(a) (solid curve). The dashed curve in Fig. 4(a) is the calculated BS (see Fig. 2), normalized also to 77 K.

For the determination of the BS as a function of the electric field, voltage pulses of 1- $\mu$ sec duration with a repetition rate of only 2 Hz have been

applied to the sample so that Joule heating is not significant. To avoid injections, bridge-shaped samples with large contact areas have been used. Results for  $(1 - \Delta U / \Delta U_s)$ , which is proportional to  $\epsilon_B$ , are plotted in Fig. 4(b) as a function of the electric field strength.  $\Delta U_s$  is the saturation value of the detector signal for high electric fields when the BS vanishes. Now the electron temperature as a function of the electric field strength is determined by comparison of Figs. 4(a) and 4(b), as indicated, and results are plotted in Fig. 5.

### III. DISCUSSION

We have performed calculations of the electron temperature, using the model given in Ref. 8, which has been modified by taking into account the degeneracy of the electron gas. In this model a Fermi distribution function in the  $\Gamma_1$  and  $L_1$  valleys with common electron temperature and energy-independent mobilities  $\mu_0$  and  $\mu_1$  in the  $\Gamma_1$  and  $L_1$  minima, respectively, were assumed. The field strength  $E$  and the electron temperature are related by an energy balance equation:

$$eE^2 \frac{\mu_0 n_0(T_e) + \mu_1 n_1(T_e)}{n} = \frac{\langle \epsilon(T_e) \rangle - \langle \epsilon(T_L) \rangle}{\tau_e}. \quad (6)$$

$\tau_e$  stands for the energy relaxation time and

$$\begin{aligned} \langle \epsilon(T_{e,L}) \rangle &= \frac{4\pi k T_{e,L}}{n} \left( \frac{2m_0 k T_{e,L}}{\hbar^2} \right)^{3/2} \\ &\times \left[ F_{3/2} \left( \frac{\epsilon_F}{k T_{e,L}} \right) + \alpha F_{3/2} \left( \frac{\epsilon_F - \Delta}{k T_{e,L}} \right) \right] + \Delta \frac{n_1}{n}. \end{aligned} \quad (7)$$

$\alpha$  is the ratio of the density of states in the  $L_1$  valleys to the density of states in the  $\Gamma_1$  minimum, and  $F_{3/2}$  are Fermi integrals. Inserting Eq. (7) and  $n_0(T_e)$  and  $n_1(T_e)$ , which were calculated above from Eqs. (2) and (3), in Eq. (6), the field strength is obtained as a function of  $T_e$ . The constants used in the calculation<sup>10,11</sup> are given in Table I. For the energy relaxation time a value of  $1.6 \times 10^{-11}$  sec was taken,<sup>7</sup> which can be justified to be nearly energy independent up to field strengths of 150 V/cm ("warm electrons"). Results of this calculation are also given in Fig. 5 (solid line).

From the reported results we conclude that measurements of the BS provide a useful tool for the determination of electron temperatures in degenerate semiconductors.

### ACKNOWLEDGMENTS

The support of Professor K. Seeger is gratefully acknowledged. We also wish to thank Dr. G. Bauer and E. Müller for helpful discussions.

<sup>†</sup>Work supported by the "Fonds zur Förderung der wissenschaftlichen Forschung," Austria, and the Ludwig Boltzmann Gesellschaft.

\*Now at Department of Physics, Lakehead University, Thunder Bay, Ontario, Canada.

<sup>1</sup>For example, G. Bauer and H. Kahlert, in Proceedings of the Tenth International Conference on Physics of Semiconductors, Cambridge, Mass., 1970 (unpublished), p. 65.

<sup>2</sup>A. Mooradian and A. L. McWhorter, in Ref. 1, p. 380.

<sup>3</sup>E. Burstein, Phys. Rev. **93**, 632 (1954).

<sup>4</sup>M. S. Shur, Phys. Letters **29A**, 490 (1969).

<sup>5</sup>W. Franz, Z. Naturforsch. **13a**, 484 (1958).

<sup>6</sup>L. V. Keldysh, Zh. Eksperim. i Teor. Fiz. **34**, 1138 (1958) [Sov. Phys. JETP **7**, 788 (1958)].

<sup>7</sup>H. Heinrich, K. Hess, W. Jantsch, and W. Pfeiler (unpublished).

<sup>8</sup>W. Jantsch, and H. Heinrich, Phys. Rev. B **3**, 420 (1971).

<sup>9</sup>V. Roberts and J. E. Quarrington, J. Electron. **1**, 152 (1952).

<sup>10</sup>C. Y. Liang, J. Appl. Phys. **39**, 3866 (1968).

<sup>11</sup>H. Piller, J. Appl. Phys. **37**, 763 (1966).

## Electronic Properties of an Amorphous Solid. I.A Simple Tight-Binding Theory

D. Weaire and M. F. Thorpe

*Becton Center, Yale University, New Haven, Connecticut 06520*

(Received 25 May 1971)

Using a simple Hamiltonian of the tight-binding type, rigorous bounds are derived for the density of states of a tetrahedrally bonded solid. These include inner bounds which define a band gap between occupied and unoccupied states. The derivation uses only the assumed perfect coordination of nearest neighbors, and so it holds for all tetrahedrally bonded crystal structures and random networks of the kind proposed for amorphous Si and Ge. Various other results are obtained for the fractional  $s$ - and  $p$ -like character of wave functions, the attainment of bounds, and other features of the density of states. A band-structure calculation for the diamond cubic structure serves as a test case.

### I. INTRODUCTION

Two broad classes of disordered systems are encountered in solid-state theory (see Fig. 1). In the case of what we shall call *quantitative* disorder, one defines a periodic array of potentials which are not identical. They may, for instance, be of two types, randomly distributed, in which case the theoretical model would be appropriate to a disordered binary alloy. On the other hand, one may define an array of potentials which are identical but not periodically positioned. One might call this *positional* disorder. Such a model would be appropriate for, say, a liquid metal.

If a positionally disordered system has the same coordination of nearest neighbors everywhere and we describe it with a Hamiltonian which involves only nearest-neighbor coordination, we have the special case of *topological* disorder. The distinction between this case and that of quantitative disorder is somewhat clearer. The matrix elements which specify the Hamiltonian are the same everywhere throughout the structure. It is the connectivity of the structure which is disordered. Such a topologically disordered Hamiltonian would seem to be an appropriate starting point for a theory of

the electronic properties of amorphous elemental semiconductors, and in the subsequent sections the model will be analyzed in detail.

The motivation for this study lies in recent experimental work<sup>1-6</sup> on amorphous Si and Ge. From the outset it was evident that these substances were highly disordered, and yet in many respects their electronic properties are closely similar to those of the corresponding crystals. In particular, a band gap between valence and conduction bands persists in the amorphous state. The extent to which such a gap contains a small density of states tailing off from the two bands is still a subject of debate. Be that as it may, this remains a remarkable experimental result.

A model for the structure of these elemental amorphous semiconductors which has gained wide acceptance is the *random network* model, in which every atom is almost perfectly tetrahedrally coordinated with its nearest neighbors. Distortions of bond lengths and angles from the values in the crystalline state are of the order of 10%, and yet the distribution of second and further neighbors is highly disordered.<sup>7</sup> It is by no means obvious that such a geometrical arrangement can be constructed in practice. However, this appears to